

1 **Massive variation of short tandem repeats with functional consequences across**
2 **strains of *Arabidopsis thaliana*.**

3

4 Maximilian O. Press¹, Rajiv C. McCoy¹, Ashley N. Hall², Joshua M. Akey¹, and Christine
5 Queitsch^{1*}

6

7 1: University of Washington Department of Genome Sciences, Seattle, WA

8 2: University of Washington Department of Molecular and Cellular Biology, Seattle, WA

9 *: to whom correspondence should be addressed: queitsch@uw.edu

10

11 Keywords: Short tandem repeat, microsatellite, quantitative genetics, selection,
12 *Arabidopsis thaliana*.

1 **Abstract**

2 Short tandem repeat (STR) mutations may be responsible for more than half of the
3 mutations in eukaryotic coding DNA, yet STR variation is rarely examined as a
4 contributor to complex traits. We assess the scope of this contribution across a
5 collection of 96 strains of *Arabidopsis thaliana* by massively parallel STR genotyping.
6 We found that 95% of examined STRs are polymorphic, with a median of six alleles per
7 STR in these strains. Modest STR expansions are found in most strains, some of which
8 have evident functional effects. For instance, three of six intronic STR expansions are
9 associated with intron retention. Coding STRs are depleted of variation relative to non-
10 coding STRs, consistent with the action of purifying selection, and some STRs show
11 hypervariable patterns consistent with diversifying selection. Finally, we detect dozens
12 of novel STR-phenotype associations that could not be detected with SNPs alone,
13 validating several with follow-up experiments. Our results demonstrate that STRs
14 comprise a large, unascertained reservoir of functionally relevant genomic variation.

15

16 **Introduction**

17 Mean rates of mutation vary within genomes by several orders of magnitude (1), from
18 $\sim 10^{-8}$ - 10^{-9} for substitutions to 10^{-3} - 10^{-4} for short tandem repeat (STR) mutations (2–4).
19 STR mutations generally occur through the addition or subtraction of repeat units. Given
20 the prevalence of STR loci in eukaryotic genomes, we would expect more *de novo* STR
21 mutations than single nucleotide substitutions in the human genome per generation (4),
22 even in exonic regions (Table 1). Thus, while the overall mutation rate is under the
23 strong control of natural selection, some loci experience many more mutations than
24 others (5). The existence of such highly mutable loci violates simplifying assumptions of
25 the infinite sites model of population genetics (6), namely that no locus mutates more
26 than once in a population, as well as quantitative genetic models assuming
27 contributions from many independent loci (7).

28

29 **Table 1.** Expected number of human mutations of various classes. Some plausible
30 scenarios are bolded.

Substitution rate ^a	STR mutation rate ^b	Exome size (bp) ^c	Exonic STRs ^d	Substitutions	STR mutations	log10(STR mutations / substitutions)
$1.2 * 10^{-8}$	10^{-5}	$3*10^8$	5000	0.36	0.05	-0.86
$1.2 * 10^{-8}$	10^{-4}	$3*10^8$	5000	0.36	0.5	0.14
$1.2 * 10^{-8}$	10^{-3}	$3*10^8$	5000	0.36	5	1.14
$1.2 * 10^{-8}$	10^{-5}	$3*10^8$	2000	0.36	0.02	-1.26
$1.2 * 10^{-8}$	10^{-4}	$3*10^8$	2000	0.36	0.2	-0.26
$1.2 * 10^{-8}$	10^{-3}	$3*10^8$	2000	0.36	2	0.74
$1.2 * 10^{-8}$	10^{-5}	$3*10^8$	1000	0.36	0.01	-1.56
$1.2 * 10^{-8}$	10^{-4}	$3*10^8$	1000	0.36	0.1	-0.56
$1.2 * 10^{-8}$	10^{-3}	$3*10^8$	1000	0.36	1	0.44

1 **a:** Rate taken from refs. (8, 9).

2 **b:** Range of rates taken from refs. (2, 10). Different rates represent different points in the range. This
3 value will vary according to the definition employed to select the set of STRs.

4 **c:** Approximate exome size taken from ref. (11).

5 **d:** According to ref. (12) there are 59,050 exonic STRs of at least three units, a very lax threshold. Values
6 shown represent different possible subsets of exonic STRs showing non-trivial mutation rates.

7

8 In spite of the large effects that STRs can have on complex traits and diseases in model
9 organisms and humans (13–15), their variation is rarely considered in genotype-
10 phenotype association studies due to technical obstacles. However, STR genotyping
11 methods of sufficient accuracy, throughput, and cost-effectiveness to ascertain STR
12 alleles at high throughput have recently become available (16–18). Studies leveraging
13 these methods suggest considerable contributions of STRs to heritable phenotypic
14 variation (16, 19).

15

16 From an evolutionary perspective, the high mutation rate and clear phenotypic effects of
17 STRs have been speculated to provide readily accessible evolutionary paths for rapid
18 adaptation (20–22). On longer time scales, the presence of highly mutable STRs within
19 coding regions appears to be maintained by selection (23–25). These observations
20 independently argue for important roles of STRs as a reservoir of functional genetic
21 variation.

22

1 In the present study, we apply massively parallel STR genotyping to a diverse panel of
2 well-characterized *A. thaliana* strains. We use these data to generate and test
3 hypotheses about the functional effects of STR variation, combining observations of
4 gene disruption by STR expansion, inferences about STR conservation, and analyses
5 of phenotypic association. Based on our results, we argue that STRs must be included
6 in any comprehensive account of phenotypically relevant genomic variation.

7

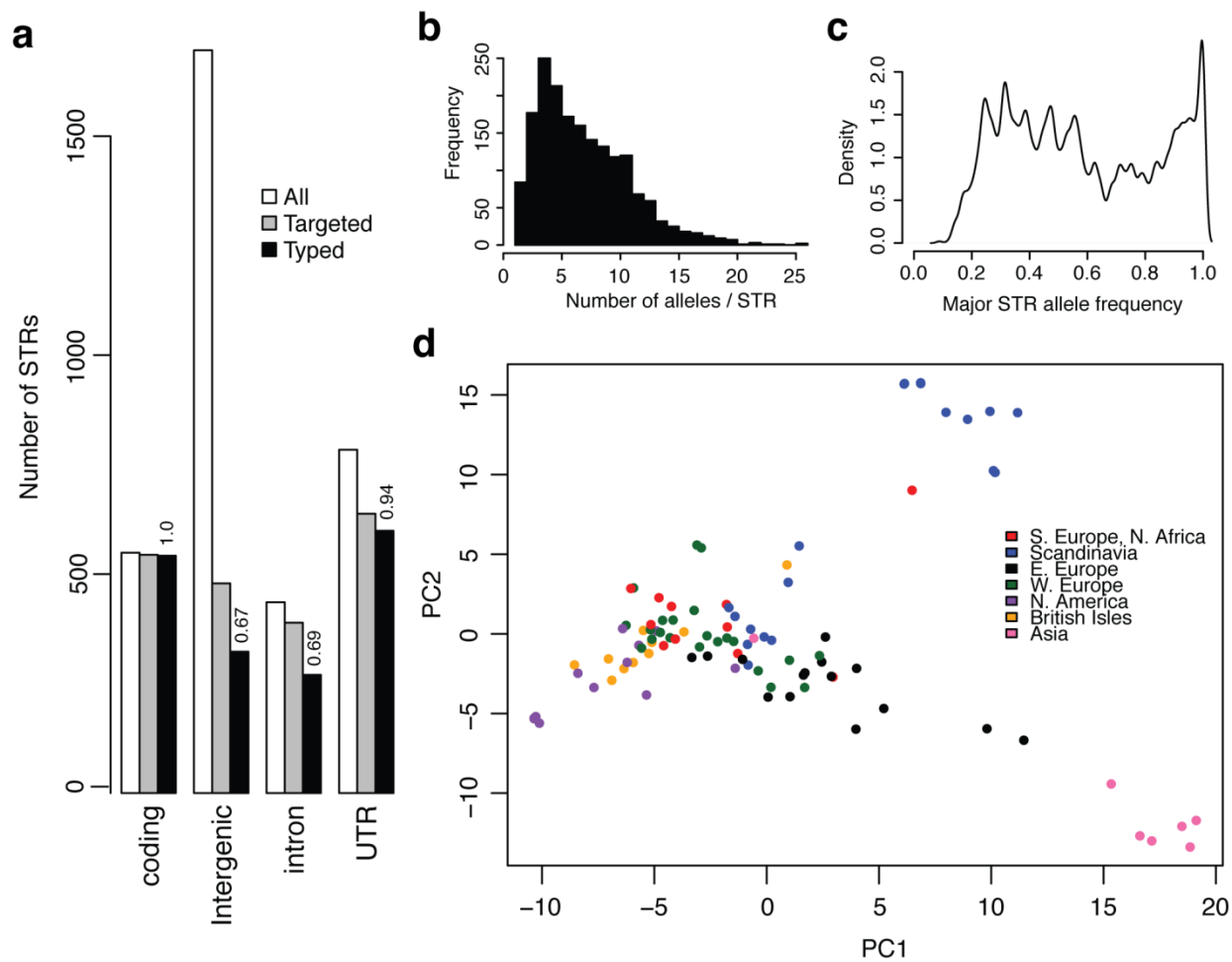
8 **Results**

9 *STR genotyping reveals complex allele frequency spectra.*

10 We targeted 2,050 STR loci for genotyping with molecular inversion probes (MIPs) (16)
11 across a core collection of 96 *A. thaliana* strains (Methods). These loci were all less
12 than 200 bp in length and had nucleotide purity of at least 90%, encompassing nearly all
13 gene-associated STRs and ~40% of intergenic STRs (Fig. 1a). We used comparisons
14 with the Col-0 reference genome, PCR analysis of selected STRs, and dideoxy
15 sequencing to estimate that MIP STR genotype calls were ~95% accurate, and
16 inaccurate calls were generally only one to two units away from the correct copy
17 number (Supplementary Note, Supplementary Fig. 1-4, Supplementary Table 1).

Press *et al.* (2017)

Massive variation of STRs in *A. thaliana*



1 **Figure 1. STRs in *A. thaliana* show a complex allele frequency distribution and geographic**
2 **differentiation.** (a): Distribution and ascertainment of STR loci. “All”: all STRs matching the
3 definition of STRs for this study, *e.g.* ≤ 180 bp length in TAIR10, $\geq 89\%$ purity in TAIR10, 2-10
4 bp nucleotide motif. “Targeted”: the 2050 STRs targeted for MIP capture. “Typed”: STRs
5 successfully genotyped in the Col-0 genome in a MIPSTR assay. Numbers above bars indicate
6 the proportion of targeted STRs in the relevant category that were successfully genotyped. (b):
7 The distribution of allele counts across all genotyped STRs. (c): The distribution of major allele
8 frequencies (frequency of the most frequent allele at each locus) across genotyped STRs. (d):
9 Principal component analysis (PCA) reveals substantial geographic structure according to STR
10 variation. PC1 and PC2 correspond, respectively, to 5.2% and 4.0% of total STR allele variance.
11
12 Across genotyped loci, we observed that 95% of STRs were polymorphic. Most STRs
13 were highly multiallelic (Fig. 1b; mean=6.4 alleles, median=6 alleles), and this variation
14 was mostly unascertained by the 1001 Genomes resource for *A. thaliana*
15 (Supplementary Fig. 3a). Coding STRs were only slightly less polymorphic (mean=4.5
16 alleles, median=4 alleles) than non-coding STRs, though it is unknown whether this

Press *et al.* (2017)

Massive variation of STRs in *A. thaliana*

1 difference is due to purifying selection or variation in mutation rates. Highlighting the
2 massive variation segregating at STR loci, 45% of STRs had a major allele with
3 frequency < 0.5. This complicates the familiar concepts of major and minor alleles,
4 which have provided a common framework for detecting genotype associations (Fig.
5 1c). Specifically, the Col-0 reference strain carries the major STR allele at only 48% of
6 STR loci. Moreover, rarefaction analysis implied that more STR alleles at these loci are
7 expected with further sampling of *A. thaliana* strains (Supplementary Fig. 4c).

8 Principal component analysis of STR variation revealed genetic structure corresponding
9 to Eurasian geography (Fig. 1d, Supplementary Fig. 5), consistent with previous
10 observations that genetic population structure is correlated with the geographic
11 distribution of *A. thaliana* (26, 27). By corroborating previous observations from a much
12 larger set of genome-wide single nucleotide polymorphism markers, this result
13 demonstrates that a comparatively small panel of STRs suffices to capture detailed
14 population structure in *A. thaliana*.

15 *Novel STR expansions are associated with splice disruptions.*

16 We next examined the frequency and functional consequences of STR expansions in *A.*
17 *thaliana*. STR expansions are high-copy-number variants of comparatively short STRs
18 that are widely recognized as contributors to human diseases (28) and other
19 phenotypes (29). While large (>150 bp) expansions are difficult to infer, we detected
20 modest STR expansions using a simple heuristic that compares the longest allele to the
21 median allele observed at each locus (Fig. 2a). We identified expansions in 64 of 96 *A.*
22 *thaliana* strains, each carrying at least one expanded STR allele from one of 28
23 expansion-prone STRs (9 coding, 6 intronic, 8 UTR, 5 intergenic). Most expansions
24 were found in multiple strains (Fig. 2b), although expansion frequency was likely
25 underestimated due to a higher rate of missing data at these loci. STR expansions
26 causing human disease can be as small as 25 copies (28), whereas we detected
27 expansions up to ~50 copies.

Press *et al.* (2017)

Massive variation of STRs in *A. thaliana*

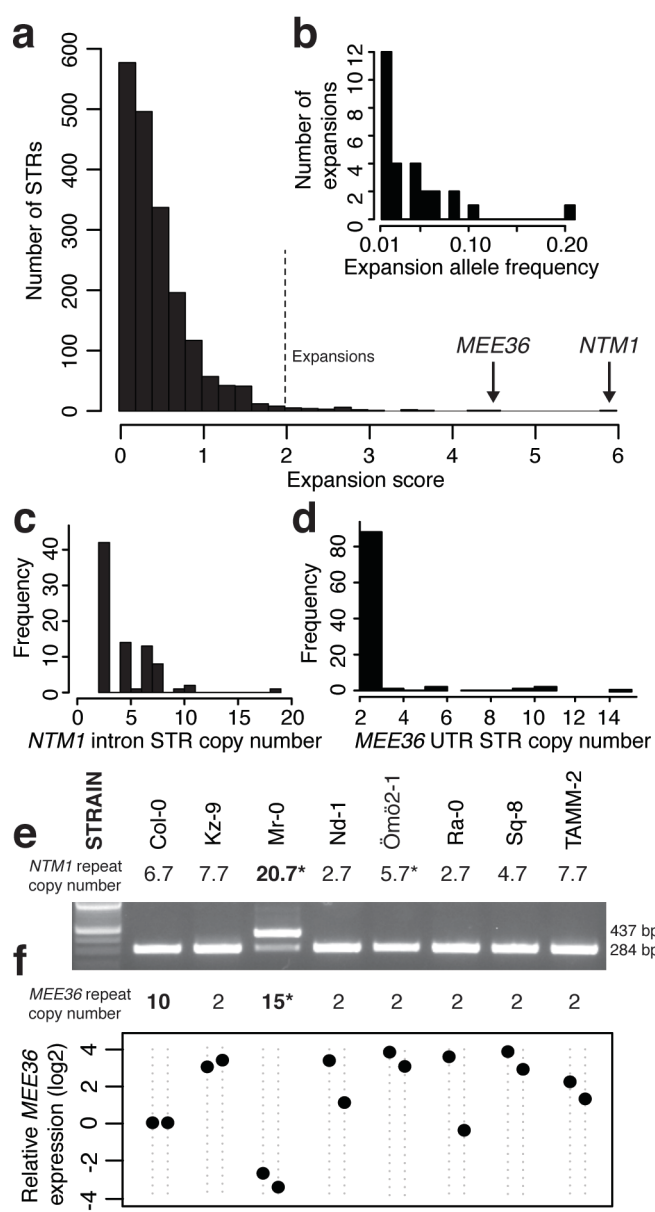


Figure 2. Inferring and assessing the functional effects of modest STR expansions. (a): The distribution of expansion scores across STRs, where the expansion score is computed as $(\max(\text{STR length}) - \text{median}(\text{STR length})) / \text{median}(\text{STR length})$. We called any STRs with a score greater than 2 a modest expansion (indicated). (b): Distribution of allele frequencies of the 28 expanded STR alleles. (c, d): Distribution of STR copy number of the intronic STR in the *NTM1* gene and the 3' UTR STR in the *MEE36* gene. (e): RT-PCR demonstrates intron retention in *NTM1* mRNA in the Mr-0 strain, which carries the STR expansion, yielding an aberrant 437-bp product. (f): *MEE36* transcript abundances measured by qRT-PCR and normalized relative to *UBC21* transcript levels. For each strain, two independent biological replicates are shown as points. Transcript levels are expressed relative to Col-0 levels (set to 1). *: STR genotype corrected by dideoxy sequencing. Strains and order are the same between (e) and (f).

We assayed the effects of STR expansions on expression of associated genes. The

Press *et al.* (2017)

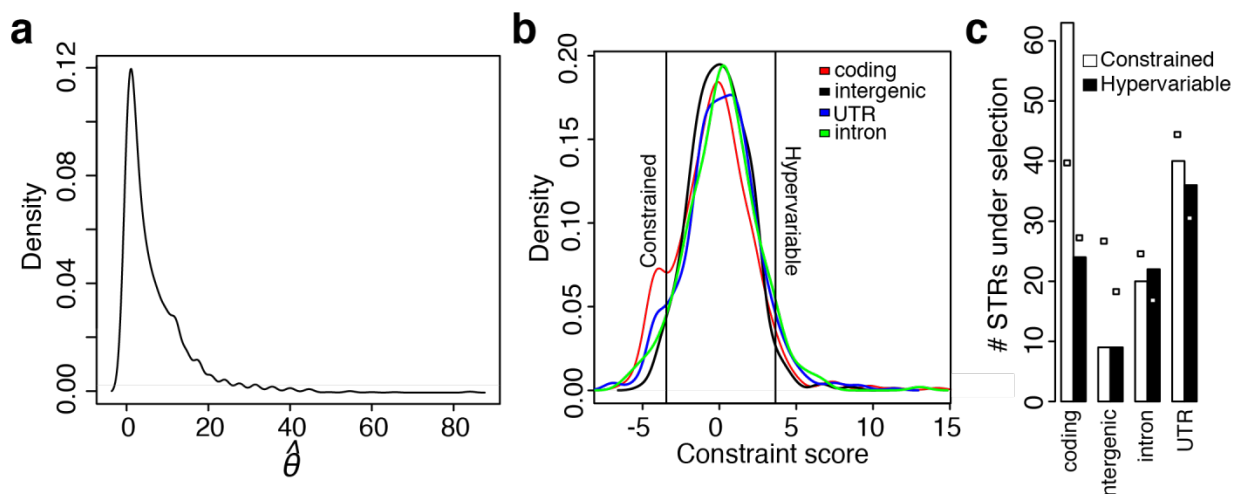
Massive variation of STRs in *A. thaliana*

1 most dramatic expansions (with large relative copy number increase) affected an
2 intronic STR in the *NTM1* gene (Fig. 2c; five other expansions also resided in introns)
3 and a STR in the 3' UTR of the *MEE36* gene (Fig. 2d). These genes, respectively, have
4 roles in cell proliferation and embryonic development. Intronic STR mutations can
5 disrupt splicing, causing altered gene function (30) and human disease (31). Therefore,
6 we assayed effects on splicing of all six expanded intronic STRs. In three cases, the
7 expanded allele was associated with partial or full retention of its intron (Supplementary
8 Fig. 6, Supplementary Note), including the major *NTM1* splice form in the Mr-0 strain
9 (Fig. 2e). We confirmed intron retentions by dideoxy sequencing of cDNA
10 (Supplementary Fig. 7a). Retention of the *NTM1* intron is predicted to lead to a
11 nonsense mutation truncating most of the *NTM1* protein (Supplementary Fig. 7b). For
12 the other two retentions, more complex and STR allele-specific mRNA species were
13 formed (Supplementary Fig. 6, Supplemental Text). The *MEE36* STR expansion alleles
14 were associated with dramatically reduced *MEE36* transcript levels (Fig. 2f), possibly
15 due to the STR expansion altering transcript processing (32). These examples
16 emphasize the potential for previously unascertained STR variation to modify gene
17 function. Moreover, we show that the distribution of allele sizes itself can be informative,
18 enabling predictions about STR functional effects.

19 *Signatures of functional constraint on STR variation.*

20 Using the observed STR allele frequency distributions, we next attempted to infer
21 selective processes acting on STRs. While previous models for evaluating functional
22 constraint on STRs are few (33), there is consensus that selection shapes STR
23 variation (21, 23, 33, 34). Naively, we would expect that coding STRs should show
24 increased constraint (lower variation). Consistent with this expectation, we observed
25 that most invariant STRs are coding (53 of 84 invariant STRs genotyped across at least
26 70 strains; odds ratio = 4.5, $p = 5 \times 10^{-11}$, Fisher's Exact Test). However, methods of
27 inferring selection by allele counting are confounded by population structure and
28 mutation rate, which vary widely across STRs in this (Fig. 3a) and other studies (3, 35).

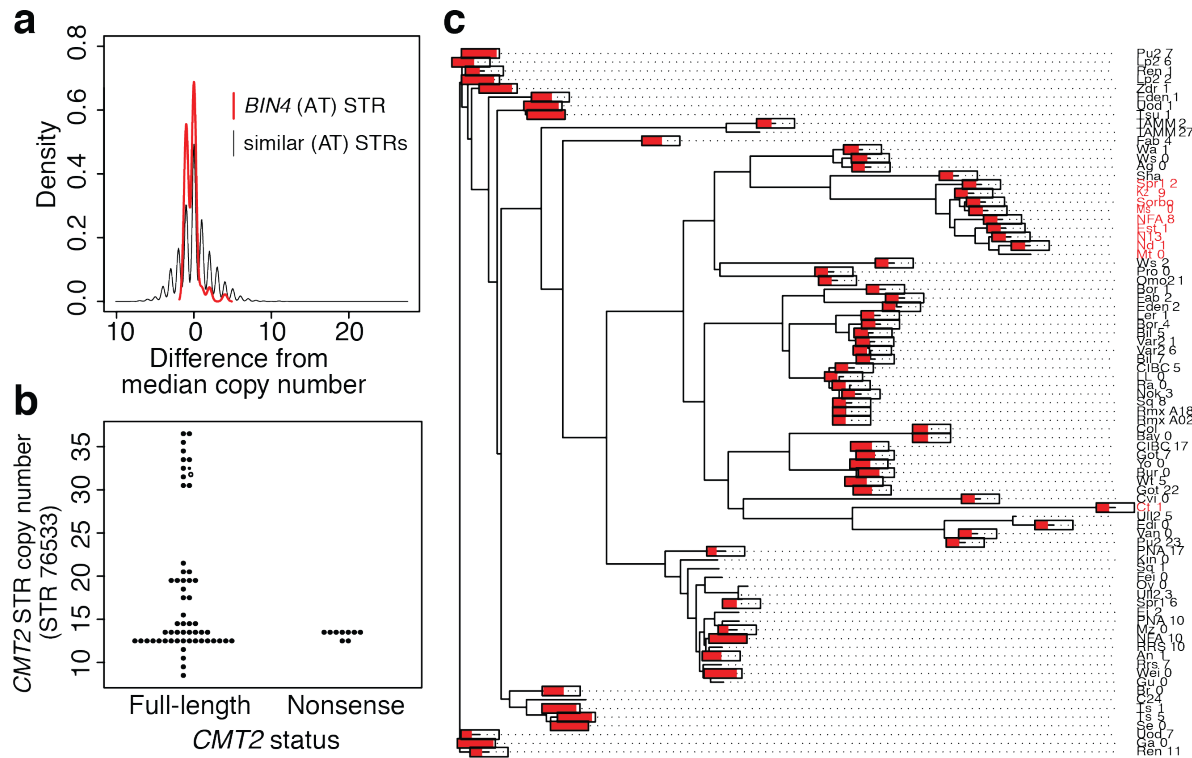
1 Therefore, to account for mutation rate and population structure, we used support vector
2 regression (SVR) to predict STR variability across these 96 strains, using well-
3 established correlates of STR variability (e.g. STR unit number and STR purity; Online
4 Methods) (3, 10, 36). Selection was defined as deviation from expected variation of a
5 neutral STR among strains. We trained SVRs on the set of intergenic STRs, which
6 should experience minimal selection relative to STRs associated with genes
7 (Supplementary Fig. 8-10). We used bootstrap aggregation of SVR models to compute
8 a putative constraint score for each STR by comparing its observed variability to the
9 expected distribution from bootstrapped SVR models (Fig. 3b, Supplementary Note,
10 Supplementary File 1).



11
12 **Figure 3. Detecting functionally constrained STRs.** (a): The distribution of $\hat{\theta}$ (estimated
13 mutation rate (6)) across all genotyped STR loci. (b): Distribution of “selection scores” across all
14 STRs, separated by locus category. Vertical lines indicate 2.5% and 97.5% quantiles of the
15 distribution of intergenic STRs, which are used as thresholds for putative constraint and
16 hypervariability respectively. (c): Constrained or hypervariable STRs separated by locus
17 category. White boxes indicate the expected numbers for each bar, based on number of STRs in
18 each locus category and number of STRs under different types of selection.

19 According to constraint scores, 132 STRs were less variable than expected under
20 neutrality, suggesting purifying selection on these loci (Fig. 3c). Among these, coding
21 STRs were overrepresented relative to their prevalence ($OR = 2.4$, $p = 3.7 \times 10^{-6}$, Fisher’s
22 Exact Test; Figure 3c); this enrichment of coding STRs among constrained STRs
23 agrees with our naïve analysis of invariant STRs above. Examples of constrained

1 coding STRs included STRs encoding homologous polylysines adjoining the histone
2 core in three different histone H2B proteins; notably, core histones are among the most
3 conserved proteins across eukaryotes. Generally, coding STRs showing purifying
4 selection encoded roughly half as many polyserines and twice as many acidic
5 homopolymers as expected from the *A. thaliana* proteome (Supplementary Table 3)
6 (37). While the interpretation of this association is unclear, it may be related to some
7 structural role of such different classes of homopolymers in proteins. Although many
8 more coding STRs are probably functionally constrained, our power to detect such
9 constraints is limited by the size of the dataset. We also observed high conservation of
10 some STRs in non-coding regions, though this is less interpretable given the ambiguous
11 relationship between sequence conservation and regulatory function in *A. thaliana* (38).
12 The most constrained intronic STR, in the *BIN4* gene, which is required for
13 endoreduplication and normal development (39), shows a restricted allele frequency
14 spectrum compared to similar STRs (Fig. 4a).



1 **Figure 4. Non-coding STRs showing non-neutral variation.** (a): *BIN4* intron STR is constrained
2 relative to similar STRs. Allele frequency spectra are normalized by subtracting the median copy
3 number (9 for the *BIN4* STR). All pure STRs with TA/AT motifs and a median copy number
4 between 7 and 12 are included in the “similar STRs” distribution. (b): Lack of association
5 between near-expansion *CMT2* STR alleles and previously described nonsense mutations. (c):
6 Neighbor-joining tree of a 10KB region of *A. thaliana* chromosome 4 encompassing the *CMT2*
7 gene across 81 strains with available data. Tip labels in red carry an adaptive nonsense
8 mutation early in the first exon of *CMT2*, as noted previously (40). Red bars drawn on tips of the
9 tree indicate the length of the *CMT2* intronic STR (as a proportion of its maximum length, 36.5
10 units). The bars are omitted for tips with missing STR data.

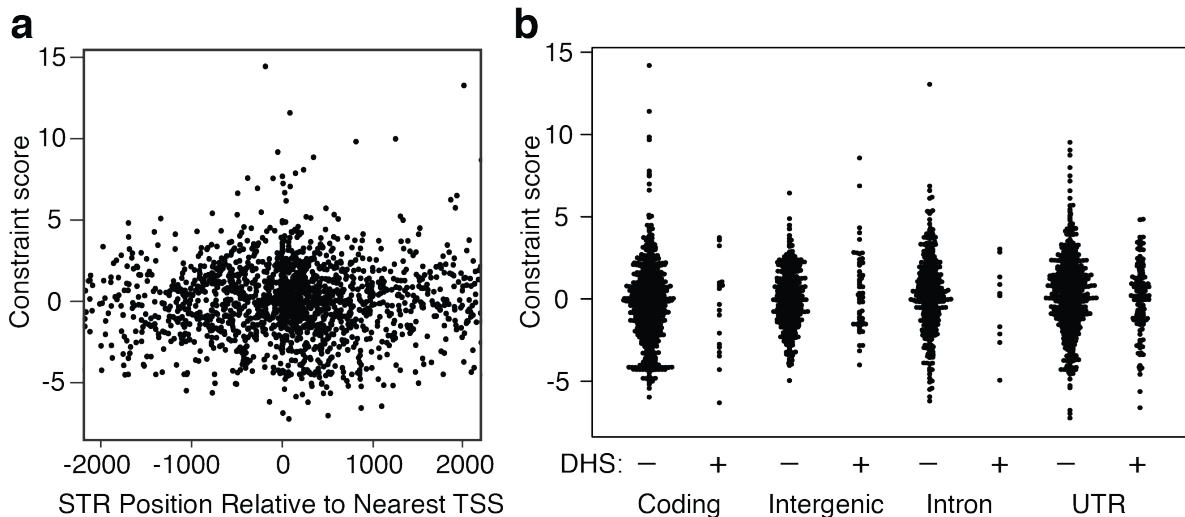
11 Hypervariable coding STRs (showing more alleles than expected) were too few for
12 statistical arguments, but nonetheless showed several notable patterns (Supplementary
13 Note, Supplementary Fig. 11). For example, 3/24 hypervariable coding STRs encoded
14 polyserines in F-box proteins, suggesting that STR variation may serve as a mechanism
15 of diversification in this protein family, which shows dramatically increased family size
16 and sequence divergence in some plant lineages (41, 42). One non-coding
17 hypervariable STR was associated with the *Chromomethylase 2* (*CMT2*) gene, which is
18 under positive selection in *A. thaliana* (40). Specifically, *CMT2* nonsense mutations in
19 some populations are associated with temperature seasonality. We considered whether
20 the extreme *CMT2* STR alleles might be associated with these nonsense mutations.
21 Instead, these extreme alleles exclusively occurred in strains with full-length *CMT2* (Fig.
22 4b). Strains with the common *CMT2* nonsense mutation form a tight clade in the *CMT2*
23 sequence tree, whereas the *CMT2* STR length fluctuates rapidly throughout the tree
24 and appears to converge on longer alleles independently in different clades (Fig. 4c).
25 These convergent changes are consistent with a model in which the *CMT2* STR is a
26 recurrent target of positive selection.

27 We further assessed whether STR conservation can be attributed to *cis*-regulatory
28 function. The abundance of STRs in eukaryotic promoters (43), and their associations
29 with gene expression (in *cis*) (19, 44), have suggested that STRs affect transcription,
30 possibly by altering nucleosome positioning (44). We examined whether STRs near
31 transcription start sites (TSSs) showed signatures of functional constraint (Fig. 5a). We
32 found little evidence for reduced STR variation near TSSs, suggesting that *cis*-

Press *et al.* (2017)

Massive variation of STRs in *A. thaliana*

1 regulatory effects do not generally constrain STR variation in *A. thaliana*. Moreover, we
2 found no relationship between constraint scores and location of STRs in accessible
3 chromatin sites marking regulatory DNA (Fig. 5b).



4

5 **Figure 5. Relationship of STR constraint to gene regulatory elements.** (a): Constraint score
6 from Figure 3b plotted with respect to nearest TSS. (b): Constraint score from Figure 3b plotted
7 with respect to STR annotations and presence of (putatively regulatory) DNase I hypersensitive
8 sites (DHS).

9 *STRs yield numerous novel genotype-phenotype associations.*

10 We next addressed the question of whether STR genotypes contribute new information
11 for explaining phenotypic variation. It is often assumed that STR phenotype
12 associations should be captured through linkage to common single nucleotide
13 polymorphisms (SNPs) (45). This assumption is inconsistent with available data. Human
14 STR data (45, 46) and simulation studies (47) indicate limited linkage disequilibrium
15 (LD) between STRs and SNPs, making it unclear whether SNP markers can
16 meaningfully tag STR genotypes. Indeed, we found little evidence of LD between STR
17 and SNPs in *A. thaliana* (Fig. 6a). Moreover, the observed LD around STR loci declined
18 with increasing STR allele number (Supplementary Fig. 12), consistent with an
19 expected higher mutation rate at multiallelic loci (6, 47). This result suggests that STR-
20 phenotype associations need to be directly tested rather than relying on linkage to

1 SNPs. *A. thaliana* offers extensive high-quality phenotype data for our inbred strains,
2 which have been previously used for SNP-based association studies (48). We tested
3 each polymorphic STR for associations across the 96 strains with each of 105 published
4 phenotypes. For the subset of 32 strains for which RNA-seq data were available (49),
5 we also tested for associations between STR genotypes and expression of genes within
6 1MB (*i.e.*, eQTLs; Supplementary Note). Although our power to detect eQTLs was
7 limited by sample size, we detected 12 significant associations. The strongest
8 association was between a STR residing in long noncoding RNA gene *AT4G07030* and
9 expression of the nearby stress-responsive gene *AtCPL1* (Supplementary Fig 13,
10 Supplementary Table 4).

11 We next focused on organismal phenotypes. Certain STRs showed associations with
12 multiple phenotypes, and flowering time phenotypes were particularly correlated with
13 one another (Fig. 6c,d). Similar to these patterns, SNPs have also shown associations
14 with multiple phenotypes, and correlated flowering time phenotypes are among the
15 strongest associations in the same strains (48). As in previous association studies using
16 STRs (19), some inflation was apparent in test p-values compared to expectations,
17 though the same tests using permuted STR genotypes showed negligible inflation (Fig.
18 6b, Supplementary Fig 14). Negligible inflation with permuted genotypes has been used
19 previously to exclude confounding from population structure (19), which we will also
20 presume here (Supplementary Note). We found 137 associations between 64 STRs and
21 25 phenotypes at stringent genome-wide significance levels (Methods; Supplementary
22 Table 5). Given the low LD observed between STRs and other variants, STR variants
23 may themselves be causal, rather than merely tagging nearby causal variants. Our
24 analysis found plausible candidate genes, such as *COL9*, which acts in flowering time
25 pathways and contains a flowering time-associated STR, and *RABA4B*, which acts in
26 the salicylic acid defense response (50) and contains a STR associated with lesion
27 formation.

Press *et al.* (2017)

Massive variation of STRs in *A. thaliana*

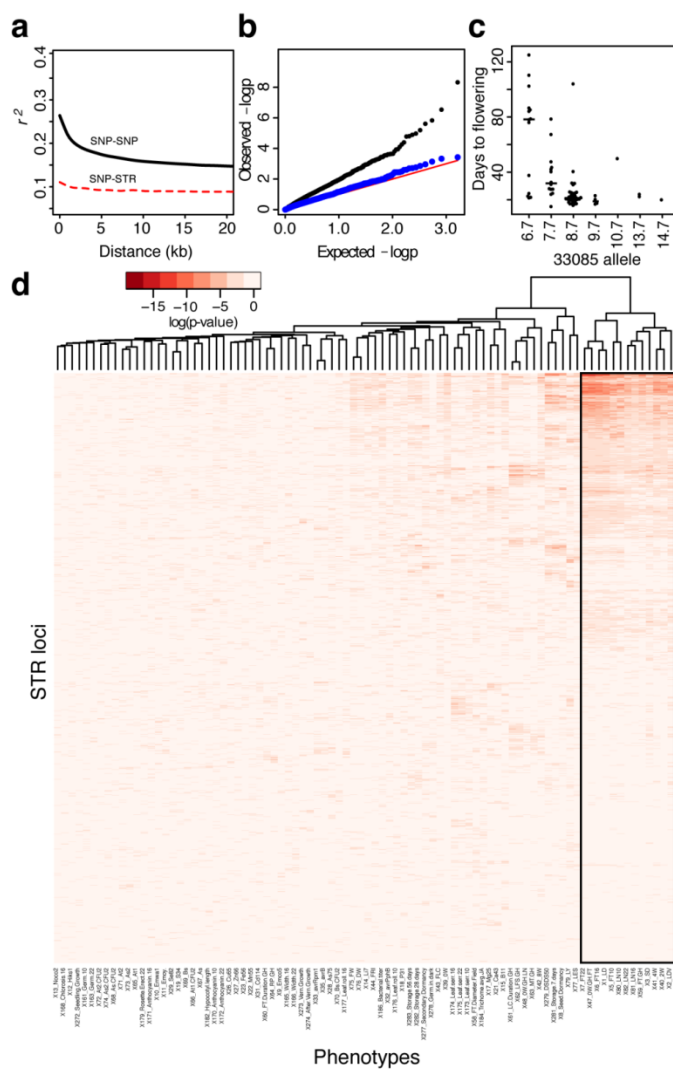


Figure 6. Diverse associations of STRs with quantitative phenotypes. (a): Multiallelic LD (51) estimates for STR and SNP loci. Lowess lines for each category are plotted. All values of $r^2 < 0.05$ are omitted from lowess calculation for visualization purposes. (b): Quantile-quantile plot of p-values from tests of association between STRs and germination rate after 28 days of storage. (c): An example association between an STR (33085) and a phenotype (flowering time in long days after 4 weeks vernalization) in *A. thaliana* strains. Median of each distribution is indicated by a bar proportional in width to the number of observations. (d): Heatmap showing pairwise associations between STRs and phenotypes, summarized by the p-value from a linear mixed model, fitting STR allele as a fixed effect and kinship as a random effect. Both rows and columns are clustered, though the row dendrogram was omitted for clarity. STRs with genotype information in fewer than 25 strains are not displayed. Flowering time phenotypes are boxed in black.

14

15 We evaluated whether these associations might have been found using SNP-based
16 analyses. We found that STR effects on phenotype are largely not accounted for by

Press *et al.* (2017)

Massive variation of STRs in *A. thaliana*

1 nearby SNP variation. Considering the strongest association for each STR, only 18 of
2 the 64 STRs were near potentially confounding SNP variants, and most associations
3 (14/18) were robust to adjustment for nearby SNP genotypes (48) (Supplementary
4 Table 6, Supplementary Note). One notable exception was a STR closely linked to a
5 well-known deletion of the *RPS5* gene in a hypervariable region of chromosome 1 (52)
6 that causes resistance to bacterial infection (53). *RPS5* status is under balancing
7 selection in *A. thaliana* (52). In this case, the association and the linkage are apparently
8 strong enough (the STR is ~4KB upstream of the deletion) that this STR tags *RPS5*'s
9 effect on infection. The observation of a STR tagging a hypervariable region leads us to
10 speculate that STR variation holds information about genomic regions with complex
11 mutational histories.

12 To assess the STR contribution to the variance of a specific trait, we performed a naïve
13 variance decomposition of the long-day flowering phenotype into SNP and STR
14 components, as represented by the loci showing associations with this trait. Our results
15 suggested that STRs potentially contribute as much or more variance than SNPs to this
16 phenotype (Supplementary Note, Supplementary Table 7). Estimated effect sizes for
17 STR variants on this phenotype were similar to those of large-effect SNP variants (48)
18 (Supplementary Fig 15).

19 Finally, we used mutant analysis to evaluate the two strongest flowering time
20 associations, a coding STR in *AGL65* and an intronic STR in the uncharacterized gene
21 *AT4G01390*; neither locus had been associated with flowering time phenotypes. We
22 found that disruptions of both STR-associated genes conferred modest early flowering
23 effects (by ~2 days and ~1 rosette leaf, $p < 0.05$ for each in linear mixed models;
24 Supplementary Fig 16), supporting the robustness of our STR-phenotype associations.
25 Taken together, our study suggests that STRs contribute substantially to phenotypic
26 variation.

27 Discussion

28 Our results imply that STRs contribute substantially to trait heritability in *A. thaliana*.

1 There is little support for the hypothesis that STRs are “junk DNA”: STRs are apparently
2 constrained by functional requirements, STR variation can disrupt gene function, and
3 STR variation is associated with phenotypic variation. Considering that STR variation is
4 represented poorly by nearby SNPs, the failure to directly ascertain STRs will mask
5 most phenotypic consequences of such STR effects. If STR variation contributes to the
6 genetic variance, as we argue here, the relevance of any genome-wide association
7 study relying on SNP genotypes alone will be limited.

8 Compared to other classes of markers, STRs may exert an outsized influence on the
9 phenotypic variance due to *de novo* mutations (V_m ; Table 1, (4)). Estimates of V_m from
10 model organisms are on the order of 1%, but may vary substantially from trait to trait
11 (54). STRs are good candidates for a substantial proportion of this variance, given their
12 high mutation rate, residence in functional regions, and functional constraint
13 demonstrated here (though we make no attempt to quantify V_m from STRs in this study).
14 In previous work (55), we showed apparent copy number conservation of a STR in spite
15 of a high mutation rate. In this case, deviation from the conserved copy number
16 produced aberrant phenotypes. Our observation that constrained STRs are common
17 suggests that STRs are a likely source of deleterious *de novo* mutations which are
18 subsequently removed by selection.

19 The extent to which STRs affect phenotype is only partially captured in this study.
20 Specifically, we assayed two STRs shown to cause phenotypic variation in prior
21 transgenic *A. thaliana* studies (29, 56), but these STR loci did not show strong
22 signatures of phenotypic association or of selection. This lack of ascertainment
23 suggests that many more functionally important STRs exist in *A. thaliana* than we can
24 detect with the analyses presented here. For example, the polyQ-encoding STR in the
25 *ELF3* gene causes dramatic variation in developmental phenotypes (56), yet we find no
26 statistical associations between this locus and phenotype across our 96 strains. In this
27 case the lack of phenotype association is expected; *ELF3* STR alleles interact
28 epistatically with several other loci (57), and thus would require increased power or
29 more sophisticated analyses to detect associations. Indeed, we have argued that STRs

Press *et al.* (2017)

Massive variation of STRs in *A. thaliana*

1 are more likely than less mutable classes of genomic variation to exhibit epistasis (13).
2 In consequence, we expect that the associations described in the present study are an
3 underestimate of STR effects on phenotype. Moreover, our data are constrained by MIP
4 technology, which limits the size and composition of STR alleles that we can ascertain
5 (Figure 1a, Supplementary Figures 1-2).

6 Considering next a mechanistic perspective, the association we observe between
7 intronic STR expansions and splice disruptions may be an important mechanism by
8 which STRs contribute to phenotypic variation. In humans, unascertained diversity of
9 splice forms contributes substantially to disease (58), and this diversity is larger than
10 commonly appreciated (59). We demonstrate that this mechanism is common at least
11 for expansions; future work should evaluate how tolerant introns are to different
12 magnitudes of STR variation, as these effects on protein function may prove to be both
13 large and relatively prevalent. The phenotypic contributions of loci with high mutation
14 rate remain underappreciated, specifically in cases where such loci are difficult to
15 ascertain with high-throughput sequencing. The results presented here argue that STRs
16 are likely to play a substantial role in phenotypic variation and heritability. Accounting for
17 the heterogeneity of different classes of genomic variation, and specifically variation in
18 mutation rate, will advance our understanding of the genotype-phenotype map and the
19 trajectory of molecular evolution.

20 **METHODS**

21 **ONLINE METHODS**

22 **Probe design**

23 We used TRF (60) (parameters: matching weight 2, mismatching penalty 5, indel penalty
24 5, match probability 0.8, indel probability 0.1, score \geq 40 and maximum period 10) to
25 identify STRs in the TAIR8 build of the *Arabidopsis thaliana* genome, identifying 7826
26 putative STR loci under 200bp (Supplementary File 2). We restricted further analysis to
27 the 2409 loci with repeat purity $\geq 89\%$. We chose 2307 STRs from among these,
28 prioritizing STRs in coding regions, introns, or untranslated regions (UTRs), higher STR

Press *et al.* (2017)

Massive variation of STRs in *A. thaliana*

1 unit purity, and expected variability (VARscore (36)). We designed (61) molecular
2 inversion probes (MIPs) targeting these STR loci in 180bp capture regions with 8bp
3 degenerate tags in the common MIP backbone. For this purpose, we converted STR
4 coordinates to the TAIR10 build and used the TAIR10 build as a reference genome. We
5 used single nucleotide variants (SNVs) in 10 diverse *Arabidopsis thaliana* strains (62) to
6 avoid polymorphic sites in designing MIP targeting arms. We filtered out MIPs
7 predicted to behave poorly (MIPGEN logistic score < 0.7), discarded MIPs targeting
8 duplicate regions, and substituted MIPs designed around SNVs as appropriate. We
9 attempted to re-design filtered MIPs with 200bp capture regions using otherwise
10 identical criteria. This yielded a final set of 2050 STR-targeting MIP probes
11 (Supplementary File 3).

12

13 **MIP and library preparation**

14 These 2050 probes were ordered from Integrated DNA Technologies as desalted DNAs
15 at the 0.2 picomole scale and resuspended in Tris-EDTA pH 8.0 (TE) to a concentration
16 of 2 μ M and stored at 4° C. We pooled and diluted probes to a final stock
17 concentration of 1 nM. We phosphorylated probes as described previously (63). We
18 performed DNA preparation from whole aerial tissue of adult *A. thaliana* plants. We
19 prepared MIP libraries essentially as described previously(16, 63) using 100 ng *A.*
20 *thaliana* genomic DNA for each of 96 *A. thaliana* strains.

21

22 **Sequencing**

23 We sequenced pooled capture libraries essentially as previously described(16) on
24 NextSeq and MiSeq instruments collecting a 250bp forward read sequencing the
25 ligation arm and captured target sequence, an 8bp index read for library
26 demultiplexing, and a 50bp reverse read sequencing the extension arm and
27 degenerate tag for single-molecule deconvolution. In each run, 10% of the sequenced
28 library pool consisted of high-complexity whole-genome library to increase sequence
29 complexity. For statistics and further details of data acquired for each library see
30 Supplementary Tables 8 and 9.

1

2 **STR annotation**

3 We annotated STRs according to Araport11 (64), classifying all STRs as coding,
4 intronic, intergenic, or UTR-localized, and indicating whether each STR overlapped
5 with transposable element sequence. To identify regulatory DNA, we used the union of
6 seven distinct DNasel-seq experiments (65) covering pooled or isolated tissue types.
7 For additional details, see the Supplementary Note.

8

9 **Sequence analysis**

10 Sequences were demultiplexed and output into FASTQ format using BCL2FASTQ
11 v2.17 (Illumina, San Diego). We performed genotype calling essentially as described
12 previously (16), with certain modifications (Supplementary Note, Supplementary Table
13 1).

14 Note that our *A. thaliana* strains are inbred, and more stringent filters and data
15 processing would be necessary to account for heterozygosity. For information about
16 comparison with the Bur-0 genome, see the Supplementary Note. Updated scripts
17 implementing the MIPSTR analysis pipeline used in this study are available at
18 https://osf.io/mv2at/?view_only=d51e180ac6324d2c92028b2bad1aef67.

19

20 **Statistical analysis and data processing**

21 We performed all statistical analysis and data exploration using R v3.2.1 (66). For plant
22 experiments, we fit mixed-effects models using Gaussian (flowering) or binomial
23 generalized linear models using experiment and position as random effects and
24 genotype as a fixed effect.

25

26 **STR expansion inference**

27 We inferred STR expansions where the maximum copy number of an STR is at least
28 three times larger than the median copy number of that STR. Various alleles of STR
29 expansions were inspected manually in BAM files. Selected cases were dideoxy-
30 sequenced and analyzed as described.

1

2 **Plant material and growth conditions**

3 Plants were grown on Sunshine soil #4 under long days (16h light : 8h dark) at 22°C
4 under cool-white fluorescent light. T-DNA insertion mutants were obtained from ABRC
5 (67) (Supplementary Table 11). For flowering time experiments, plants were grown in
6 36-pot or 72-pot flats; days to flowering (DTF) and rosette leaf number at flowering
7 (RLN) were recorded when inflorescences were 1cm high. Results are combined
8 across at least three experiments.

9

10 **Gene expression and splicing analysis**

11 We grew bulk seedlings of indicated strains on soil for 10 days, harvested at Zeitgeber
12 time 12 (ZT12), froze samples immediately in liquid nitrogen, and stored samples at -
13 80°C until further processing. We extracted RNA from plant tissue using the SV RNA
14 Isolation kit (including DNase step; Promega, Madison, WI), and subsequently treated it
15 with a second DNase treatment using the Turbo DNA-free kit (Ambion, Carlsbad, CA).
16 We performed cDNA synthesis on ~500ng RNA for each sample with oligo-dT adaptors
17 using the RevertAid kit (ThermoFisher, Carlsbad, CA). We performed PCR analysis of
18 cDNA with indicated primers (Supplementary Table 10) and ~25 ng cDNA with the
19 following protocol: denaturation at 95° 5 minutes, then 30 cycles of 95° 30 seconds,
20 55° 30 seconds, 72° 90 seconds, ending with a final extension step for 5 minutes at
21 72°. We gel-purified and sequenced electrophoretically distinguishable splice variants
22 associated with STR expansions. Each RT-PCR experiment was performed at least
23 twice with different biological replicates.

24

25 **Population genetic analyses**

26 For PCA, STRs with missing data across the 96 strains were omitted, leaving 987 STRs
27 with allele calls for every strain. $\hat{\theta}$ was estimated using the approximation $\hat{\theta} = \frac{1}{8\bar{X}^2} - 0.5$,
28 (6) where \bar{X} is the average frequency of all STR alleles at a locus. We computed
29 multiallelic linkage disequilibrium estimates for SNP-SNP and SNP-STR locus pairs
30 using MCLD (51). We downloaded array SNP data for the same lines (TAIR9

Press *et al.* (2017)

Massive variation of STRs in *A. thaliana*

1 coordinates) from http://bergelson.uchicago.edu/wp-content/uploads/2015/04/call_method_75.tar.gz (68). For each locus, both SNP and
2 STR, we computed linkage disequilibrium scores with 150 surrounding loci. To
3 facilitate comparison, we computed lowess estimates of linkage only for those locus
4 pairs in the plotted distance window in each case, and only for locus pairs with $r^2 >$
5 0.05.

6

7 **Inference of conservation**

8 STRs typed across 70 *A. thaliana* strains or fewer were dropped from this analysis, as
9 the estimates of their variability were unlikely to be accurate, leaving 1825 STRs. We
10 measured STR variation as the base-10 logarithm of the standard deviation of STR
11 copy number (Supplementary Note). We used bootstrap aggregation (“bagging”) to
12 describe a distribution of predictions as follows. An ensemble of 1000 support vector
13 regression (SVR, fit using the *ksvm()* function in the kernlab package(69)) models was
14 used to predict expected neutral variation of each STR as quantified by each measure
15 (Supplementary Note). We used this distribution of bootstrapped predictions for
16 intergenic STRs to compute putative conservation scores (Z-scores) for each STR.
17 Scores below the 2.5% ($Z < -3.46$) and above the 97.5% ($Z > 3.65$) quantiles of
18 intergenic STRs were considered to be putatively constrained and hypervariable
19 respectively.

20

21 **eQTL inference**

22 We downloaded normalized transcriptome data for *A. thaliana* strains from NCBI GEO
23 GSE80744 (49). We used the Matrix eQTL package (70) to detect associations, fitting
24 also 10 principal components from SNP genotypes to correct for population structure.
25 Following precedent (19), we fitted additive models assuming that STR effects on
26 expression would be a function of STR copy number. We used Kruskal-Wallis rank-
27 sum tests to test the null hypothesis of no association following correction.

28

29 **Genotype-phenotype associations**

Press *et al.* (2017)

Massive variation of STRs in *A. thaliana*

1 We downloaded phenotype data from https://github.com/Gregor-Mendel-Institute/atpolydb/blob/master/miscellaneous_data/phenotype_published_raw.tsv. We
2 followed precedent (48) in log-transforming certain phenotypes. In all analyses we
3 treated STRs as factorial variables (to avoid linearity assumptions) in a linear mixed-
4 effect model analysis to fit STR allele effects on phenotype as fixed effects while
5 modeling the identity-by-state kinship matrix between strains (computed from SNP
6 data) as a correlation structure for strain random effects on phenotype. We performed
7 this modeling using the *lmeKin()* function from the *coxme* R package (71). We repeated
8 every analysis using permuted STR genotypes as a negative control to evaluate p-
9 value inflation, and discarded traits showing such inflation. We used $p < 10^{-6}$ as a
10 genome-wide significance threshold commensurate to the size of the *A. thaliana*
11 genome and the data at hand. For flowering time phenotypes we used a more stringent
12 $p < 10^{-10}$ threshold, as these phenotypes showed somewhat shifted p-value
13 distributions (which were nonetheless inconsistent with inflation, according to negative
14 controls). We identified potentially confounding SNP associations using the
15 <https://gwas.gmi.oeaw.ac.at/#/study/1/phenotypes> resource, using the criterion that a
16 SNP association must have a $p \leq 10^{-4}$ and be within roughly 100KB of the STR to be
17 considered. We fit models including SNPs as fixed effects as before, and performed
18 model selection using AICc (72). Additional details about association analyses are in
19 the Supplementary Note.

21

22 **Data and code availability**

23 MIP sequencing data are available in FASTQ format at the Sequence Read Archive,
24 under project number PRJNA388228. Analysis scripts are provided at
25 https://osf.io/5jm2c/?view_only=324129c85b3448a8bd6086263345c7b0, along with
26 data sufficient to reproduce analyses.

27

28 **ACKNOWLEDGMENTS**

29 We thank Keisha Carlson, Alberto Rivera, and members of the Queitsch lab for
30 technical assistance and important conversations. We thank Evan Boyle, Choli Lee,

1 Matthew Snyder, and Jay Shendure for assistance and advice concerning MIP design
2 and use. We thank the Dunham Lab and the Fields Lab for access to and help with
3 sequencing instruments. We thank UW Genome Sciences Information Technology for
4 high-performance computing resources. This work was supported in part by NIH New
5 Innovator Award DP2OD008371 to CQ.

1 **References**

- 2 1. Acuna-Hidalgo R, Veltman JA, Hoischen A (2016) New insights into the generation and role
3 of de novo mutations in health and disease. *Genome Biol* 17:241.
- 4 2. Sun JX, et al. (2012) A direct characterization of human mutation based on microsatellites.
5 *Nat Genet* 44(10):1161–5.
- 6 3. Gymrek M, Willems T, Erlich Y, Reich DE (2016) A framework to interpret short tandem
7 repeat variation in humans. *bioRxiv*:92734.
- 8 4. Willems T, et al. (2016) Population-Scale Sequencing Data Enable Precise Estimates of Y-
9 STR Mutation Rates. *Am J Hum Genet* 98(5):919–933.
- 10 5. Harpak A, Bhaskar A, Pritchard JK (2016) Mutation Rate Variation is a Primary Determinant
11 of the Distribution of Allele Frequencies in Humans. *PLOS Genet* 12(12):e1006489.
- 12 6. Haasl RJ, Payseur BA (2010) The Number of Alleles at a Microsatellite Defines the Allele
13 Frequency Spectrum and Facilitates Fast Accurate Estimation of θ . *Mol Biol Evol*
14 27(12):2702–2715.
- 15 7. Yang J, et al. (2010) Common SNPs explain a large proportion of the heritability for human
16 height. *Nat Genet* 42(7):565–9.
- 17 8. Campbell CD, et al. (2012) Estimating the human mutation rate using autozygosity in a
18 founder population. *Nat Genet* 44(11):1277–1281.
- 19 9. Kong A, et al. (2012) Rate of de novo mutations, father’s age, and disease risk. *Nature*
20 488(7412):471–475.
- 21 10. Eckert KA, Hile SE (2009) Every microsatellite is different: Intrinsic DNA features dictate
22 mutagenesis of common microsatellites present in the human genome. *Mol Carcinog*
23 48(4):379–88.
- 24 11. Ng SB, et al. (2009) Targeted capture and massively parallel sequencing of 12 human
25 exomes. *Nature* 461(7261):272–276.
- 26 12. Payseur BA, Jing P, Haasl RJ (2011) A Genomic Portrait of Human Microsatellite
27 Variation. *Mol Biol Evol* 28(1):303–312.
- 28 13. Press MO, Carlson KD, Queitsch C (2014) The overdue promise of short tandem repeat
29 variation for heritability. *Trends Genet* 30(11):504–512.
- 30 14. Fondon JW, Hammock EAD, Hannan AJ, King DG (2008) Simple sequence repeats:
31 genetic modulators of brain function and behavior. *Trends Neurosci* 31(7):328–34.
- 32 15. Hannan AJ (2010) Tandem repeat polymorphisms: modulators of disease susceptibility and
33 candidates for “missing heritability”. *Trends Genet* 26(2):59–65.

- 1 16. Carlson KD, et al. (2015) MIPSTR: A method for multiplex genotyping of germline and
- 2 somatic STR variation across many individuals. *Genome Res* 125(5):750–761.
- 3 17. Willems T, Zielinski D, Gordon A, Gymrek M, Erlich Y (2016) Genome-wide profiling of
- 4 heritable and de novo STR variations. *bioRxiv*:77727.
- 5 18. Highnam G, et al. (2013) Accurate human microsatellite genotypes from high-throughput
- 6 resequencing data using informed error profiles. *Nucleic Acids Res* 41(1):e32.
- 7 19. Gymrek M, et al. (2015) Abundant contribution of short tandem repeats to gene expression
- 8 variation in humans. *Nat Genet* 48(1):22–29.
- 9 20. Moxon ER, Rainey PB, Nowak MA, Lenski RE (1994) Adaptive evolution of highly
- 10 mutable loci in pathogenic bacteria. *Curr Biol* 4(1):24–33.
- 11 21. King DG (2012) Indirect selection of implicit mutation protocols. *Ann N Y Acad Sci*
- 12 1267:45–52.
- 13 22. Gemayel R, Vinces MD, Legendre M, Verstrepen KJ (2010) Variable tandem repeats
- 14 accelerate evolution of coding and regulatory sequences. *Annu Rev Genet* 44:445–77.
- 15 23. Mularoni L, Ledda A, Toll-Riera M, Albà MM (2010) Natural selection drives the
- 16 accumulation of amino acid tandem repeats in human proteins. *Genome Res* 20(6):745–54.
- 17 24. Yu F, et al. (2005) Positive selection of a pre-expansion CAG repeat of the human SCA2
- 18 gene. *PLoS Genet* 1(3):e41.
- 19 25. Sawaya SM, Lennon D, Buschiazzo E, Gemmell N, Minin VN (2012) Measuring
- 20 microsatellite conservation in mammalian evolution with a phylogenetic birth-death model.
- 21 *Genome Biol Evol* 4(6):636–47.
- 22 26. Nordborg M, et al. (2005) The pattern of polymorphism in *Arabidopsis thaliana*. *PLoS Biol*
- 23 3(7):e196.
- 24 27. Alonso-Blanco C, et al. (2016) 1,135 Genomes Reveal the Global Pattern of Polymorphism
- 25 in *Arabidopsis thaliana*. *Cell* 0(0). doi:10.1101/j.cell.2016.05.063.
- 26 28. Usdin K (2008) The biological effects of simple tandem repeats: Lessons from the repeat
- 27 expansion diseases. *Genome Res* 18(7):1011–1019.
- 28 29. Sureshkumar S, et al. (2009) A genetic defect caused by a triplet repeat expansion in
- 29 *Arabidopsis thaliana*. *Science* 323(5917):1060–3.
- 30 30. Li Y-C, Korol AB, Fahima T, Nevo E (2004) Microsatellites Within Genes: Structure,
- 31 Function, and Evolution. *Mol Biol Evol* 21(6):991–1007.
- 32 31. Ranum LPW, Day JW (2002) Dominantly inherited, non-coding microsatellite expansion
- 33 disorders. *Curr Opin Genet Dev* 12(3):266–271.

- 1 32. Jackson RJ (1993) Cytoplasmic regulation of mRNA function: The importance of the 3'
2 untranslated region. *Cell* 74(1):9–14.
- 3 33. Haasl RJ, Payseur BA (2013) Microsatellites as targets of natural selection. *Mol Biol Evol*
4 30(2):285–98.
- 5 34. Huntley MA, Clark AG (2007) Evolutionary Analysis of Amino Acid Repeats across the
6 Genomes of 12 *Drosophila* Species. *Mol Biol Evol* 24(12):2598–2609.
- 7 35. Schlötterer C, Kauer M, Dieringer D (2004) Allele Excess at Neutrally Evolving
8 Microsatellites and the Implications for Tests of Neutrality. *Proc Biol Sci* 271(1541):869–
9 874.
- 10 36. Legendre M, Pochet N, Pak T, Verstrepen KJ (2007) Sequence-based estimation of
11 minisatellite and microsatellite repeat variability. *Genome Res* 17(12):1787–96.
- 12 37. Karlin S, Brocchieri L, Bergman A, Mrazek J, Gentles AJ (2002) Amino acid runs in
13 eukaryotic proteomes and disease associations. *Proc Natl Acad Sci U S A* 99(1):333–8.
- 14 38. Alexandre CM, et al. (2017) Regulatory DNA in *A. thaliana* can tolerate high levels of
15 sequence divergence. *bioRxiv*:104323.
- 16 39. Breuer C, et al. (2007) BIN4, a Novel Component of the Plant DNA Topoisomerase VI
17 Complex, Is Required for Endoreduplication in *Arabidopsis*. *Plant Cell* 19(11):3655–3668.
- 18 40. Shen X, et al. (2014) Natural CMT2 Variation Is Associated With Genome-Wide
19 Methylation Changes and Temperature Seasonality. *PLOS Genet* 10(12):e1004842.
- 20 41. Xu G, Ma H, Nei M, Kong H (2009) Evolution of F-box genes in plants: Different modes
21 of sequence divergence and their relationships with functional diversification. *Proc Natl
22 Acad Sci* 106(3):835–840.
- 23 42. Clark RM, et al. (2007) Common Sequence Polymorphisms Shaping Genetic Diversity in
24 *Arabidopsis thaliana*. *Science* 317(5836):338–342.
- 25 43. Sawaya S, et al. (2013) Microsatellite tandem repeats are abundant in human promoters and
26 are associated with regulatory elements. *PloS One* 8(2):e54710.
- 27 44. Vinces MD, Legendre M, Caldara M, Hagihara M, Verstrepen KJ (2009) Unstable tandem
28 repeats in promoters confer transcriptional evolvability. *Science* 324(5931):1213–6.
- 29 45. Payseur BA, Place M, Weber JL (2008) Linkage disequilibrium between STRPs and SNPs
30 across the human genome. *Am J Hum Genet* 82(5):1039–50.
- 31 46. Willems TF, Gymrek M, Highnam G, Mittelman D, Erlich Y (2014) The landscape of
32 human STR variation. *Genome Res*:gr.177774.114–

- 1 47. Sawaya S, Jones M, Keller M (2015) *Linkage disequilibrium between single nucleotide*
2 *polymorphisms and hypermutable loci* (Cold Spring Harbor Labs Journals).
- 3 48. Atwell S, et al. (2010) Genome-wide association study of 107 phenotypes in *Arabidopsis*
4 *thaliana* inbred lines. *Nature* 465(7298):627–31.
- 5 49. Kawakatsu T, et al. (2016) Epigenomic Diversity in a Global Collection of *Arabidopsis*
6 *thaliana* Accessions. *Cell* 166(2):492–505.
- 7 50. Antignani V, et al. (2015) Recruitment of PLANT U-BOX13 and the PI4K β 1/ β 2
8 Phosphatidylinositol-4 Kinases by the Small GTPase RabA4B Plays Important Roles
9 during Salicylic Acid-Mediated Plant Defense Signaling in *Arabidopsis*. *Plant Cell*
10 27(1):243–261.
- 11 51. Zaykin DV, Pudovkin A, Weir BS (2008) Correlation-Based Inference for Linkage
12 Disequilibrium With Multiple Alleles. *Genetics* 180(1):533–545.
- 13 52. Tian D, Araki H, Stahl E, Bergelson J, Kreitman M (2002) Signature of balancing selection
14 in *Arabidopsis*. *Proc Natl Acad Sci* 99(17):11525–11530.
- 15 53. Karasov TL, et al. (2014) The long-term maintenance of a resistance polymorphism through
16 diffuse interactions. *Nature* 512(7515):436–440.
- 17 54. Lynch M (1988) The rate of polygenic mutation. *Genet Res* 51(2):137–148.
- 18 55. Rival P, et al. (2014) The conserved PFT1 tandem repeat is crucial for proper flowering in
19 *Arabidopsis thaliana*. *Genetics* 198(2):747–754.
- 20 56. Undurraga SF, et al. (2012) Background-dependent effects of polyglutamine variation in the
21 *Arabidopsis thaliana* gene ELF3. *Proc Natl Acad Sci U S A* 109(47):19363–19367.
- 22 57. Press MO, Queitsch C (2016) Variability in a Short Tandem Repeat Mediates Complex
23 Epistatic Interactions in *Arabidopsis thaliana*. *Genetics:genetics*.116.193359.
- 24 58. Cummings BB, et al. (2017) Improving genetic diagnosis in Mendelian disease with
25 transcriptome sequencing. *Sci Transl Med* 9(386):eaal5209.
- 26 59. Nellore A, et al. (2016) Human splicing diversity and the extent of unannotated splice
27 junctions across human RNA-seq samples on the Sequence Read Archive. *Genome Biol*
28 17:266.
- 29 60. Benson G (1999) Tandem repeats finder: a program to analyze DNA sequences. *Nucleic*
30 *Acids Res* 27(2):573–580.
- 31 61. Boyle EA, O’Roak BJ, Martin BK, Kumar A, Shendure J (2014) MIPgen: optimized
32 modeling and design of molecular inversion probes for targeted resequencing.
33 *Bioinformatics* 30(18):2670–2672.

- 1 62. Gan X, et al. (2011) Multiple reference genomes and transcriptomes for *Arabidopsis*
2 *thaliana*. *Nature* 477(7365):419–23.
- 3 63. Hiatt JB, Pritchard CC, Salipante SJ, O’Roak BJ, Shendure J (2013) Single molecule
4 molecular inversion probes for targeted, high-accuracy detection of low-frequency
5 variation. *Genome Res* 23(5):843–54.
- 6 64. Cheng C-Y, et al. (2017) Araport11: a complete reannotation of the *Arabidopsis thaliana*
7 reference genome. *Plant J Cell Mol Biol* 89(4):789–804.
- 8 65. Sullivan AM, et al. (2014) Mapping and Dynamics of Regulatory DNA and Transcription
9 Factor Networks in *A. thaliana*. *Cell Rep* 8(6):2015–30.
- 10 66. R Core Team (2016) *R: A Language and Environment for Statistical Computing* (R
11 Foundation for Statistical Computing, Vienna, Austria) Available at: <http://www.r-project.org/>.
- 13 67. Alonso JM, et al. (2003) Genome-wide insertional mutagenesis of *Arabidopsis thaliana*.
14 *Science* 301(5633):653–7.
- 15 68. Horton MW, et al. (2012) Genome-wide patterns of genetic variation in worldwide
16 *Arabidopsis thaliana* accessions from the RegMap panel. *Nat Genet* 44(2):212–216.
- 17 69. Karatzoglou A, Smola A, Hornik K (2016) *kernlab: Kernel-Based Machine Learning Lab*
18 Available at: <https://cran.r-project.org/web/packages/kernlab/index.html> [Accessed January
19 11, 2017].
- 20 70. Shabalin AA (2012) Matrix eQTL: ultra fast eQTL analysis via large matrix operations.
21 *Bioinformatics* 28(10):1353–1358.
- 22 71. Therneau TM (2015) *coxme: Mixed Effects Cox Models* Available at: <https://cran.r-project.org/web/packages/coxme/index.html> [Accessed January 11, 2017].
- 24 72. Hurvich CM, Tsai C-L (1989) Regression and time series model selection in small samples.
25 *Biometrika* 76(2):297–307.
- 26